

in the measurement of fluxmeter frequencies and reaction angle were smaller than the uncertainty in determining the position of one-third height of the peaks. The square root of the sum of the squares of all these errors for a typical set of measurements is quoted in Table I as the error.

These results confirm the existence of the levels at

5.96 and 6.26 Mev and show an additional level, previously unreported, at 6.18 Mev.

The authors thanks are tendered to Professor W. W. Buechner, Dr. C. P. Browne, and Mr. A. Sperduto for help and advice during the experiment, and to Mr. W. A. Tripp and Miss Janet Frothingham for scanning many of the numerous photographic plates.

PHYSICAL REVIEW

VOLUME 96, NUMBER 5

DECEMBER 1, 1954

## Angular Distribution of Protons from $(d,p)$ Reactions on $\text{Be}^9$ , $\text{N}^{14}$ , and $\text{Zn}^{68\dagger*\ddagger}$

F. S. EBY§

*University of Illinois, Urbana, Illinois*

(Received August 4, 1954)

The  $(d,p)$  stripping theory of Butler has been employed in the interpretation of the angular distributions of protons resulting from the bombardment of foil targets of  $\text{Be}^9$ ,  $\text{N}^{14}$ , and  $\text{Zn}^{68}$  by 11.9-Mev deuterons. A NaI(Tl) scintillation counter was used to detect protons emitted between angles of  $5^\circ$  and  $90^\circ$ , and pulses were recorded on a 35-mm film strip for pulse height analysis. The distribution of protons from the reaction  $\text{N}^{14}(d,p)\text{N}^{15}$  leaving  $\text{N}^{15}$  in its doublet first excited state was found to have a peak in the forward direction, indicating that the conclusion previously reached, i.e., that high momentum transfers are involved in this reaction, is probably incorrect. Although it was not possible to do so in the present work, it appears that stripping theory might be used to account for the proton distribution from this reaction if deuterons of higher energy were used. The orbital momenta of a pair of isomeric levels in the nucleus  $\text{Zn}^{69}$  as determined from the proton distributions and stripping theory are in agreement with the shell model assignments of  $p_{1/2}$  for the ground state and  $g_{9/2}$  for the 436-kev level. Higher excited levels of  $\text{Zn}^{69}$  are indicated at about 770 kev and 1.6 Mev. The distribution of the proton group leaving the final nucleus with an excitation of 770 kev is characterized by a momentum transfer,  $l_n=2$ . The  $Q$  value for the reaction leaving  $\text{Zn}^{69}$  in the ground state was determined to be  $4.16 \pm 0.15$  Mev.

### I. INTRODUCTION

THE reaction chamber and experimental arrangement which are described in the first part of this paper have been used to study the angular distributions of proton groups resulting from the deuteron bombardment of thin targets of  $\text{Be}^9$ ,  $\text{N}^{14}$ , and  $\text{Zn}^{68}$ . Previous investigations of proton distributions from  $(d,p)$  reactions on  $\text{Be}^9$  have been made at deuteron energies of 3.6 Mev,<sup>1</sup> 7.7 Mev,<sup>2</sup> 8 Mev,<sup>3</sup> and 14.5 Mev,<sup>4</sup> as well as 18 energies between 300 kev and 1.3 Mev. The present work was carried out with 11.9-Mev deuterons, and the proton groups associated with the ground state and the first excited state of  $\text{Be}^{10}$  were observed at laboratory

angles between  $5^\circ$  and  $85^\circ$ . In an earlier experimental study of the reaction  $\text{N}^{14}(d,p)\text{N}^{15}$  with 8-Mev deuterons,<sup>5</sup> the proton group associated with the doublet first excited state of  $\text{N}^{15}$  was shown to have a nearly isotropic distribution. This result has been interpreted by Butler<sup>6</sup> as indicating that the reaction proceeds primarily through the formation of a compound nucleus with little or no contribution from a stripping process. It was considered worth-while to investigate this reaction again using a higher deuteron energy and to extend the measurements to lower angles.

The successful use of stripping theory in interpreting the angular distributions of protons from  $(d,p)$  reactions has been restricted almost entirely to relatively light nuclei. Reactions involving the target nucleus  $\text{Sr}^{88}$  have been investigated by Holt and Marsham<sup>7</sup> and were found to lead to complex proton distributions which could not be explained in a simple way in terms of stripping theory. In the present work  $(d,p)$  reactions on  $\text{Zn}^{68}$  were studied for the purpose of comparing the results obtained from an interpretation of the proton distributions in terms of stripping theory with information which can be inferred from other knowledge about

† This investigation was supported jointly by the U. S. Atomic Energy Commission and the Office of Naval Research.

\* This paper is based on a thesis submitted in partial fulfillment of the requirements for the degree of Doctor of Philosophy at the University of Illinois.

‡ A preliminary report of part of this work was given at the Chicago meeting of the American Physical Society in November, 1953 [Phys. Rev. **93**, 925(A) (1954)].

§ Now at the University of California Radiation Laboratory, Livermore, California.

<sup>1</sup> Fulbright, Bruner, Bromley, and Goldman, Phys. Rev. **88**, 700 (1952).

<sup>2</sup> F. A. El-Bedewi, Proc. Phys. Soc. (London) **A65**, 64 (1952).

<sup>3</sup> J. R. Holt and T. N. Marsham, Proc. Phys. Soc. (London) **A66**, 1032 (1953) contains references to previous work.

<sup>4</sup> C. F. Black, Phys. Rev. **87**, 205(A) (1952). See also U. S. Atomic Energy Commission Report AECU 2128, 1952 (unpublished).

<sup>5</sup> W. M. Gibson and E. E. Thomas, Proc. Roy. Soc. (London) **A210**, 543 (1951).

<sup>6</sup> S. T. Butler, Proc. Roy. Soc. (London) **A208**, 559 (1951).

<sup>7</sup> J. R. Holt and T. N. Marsham, Proc. Phys. Soc. (London) **A66**, 565 (1953).

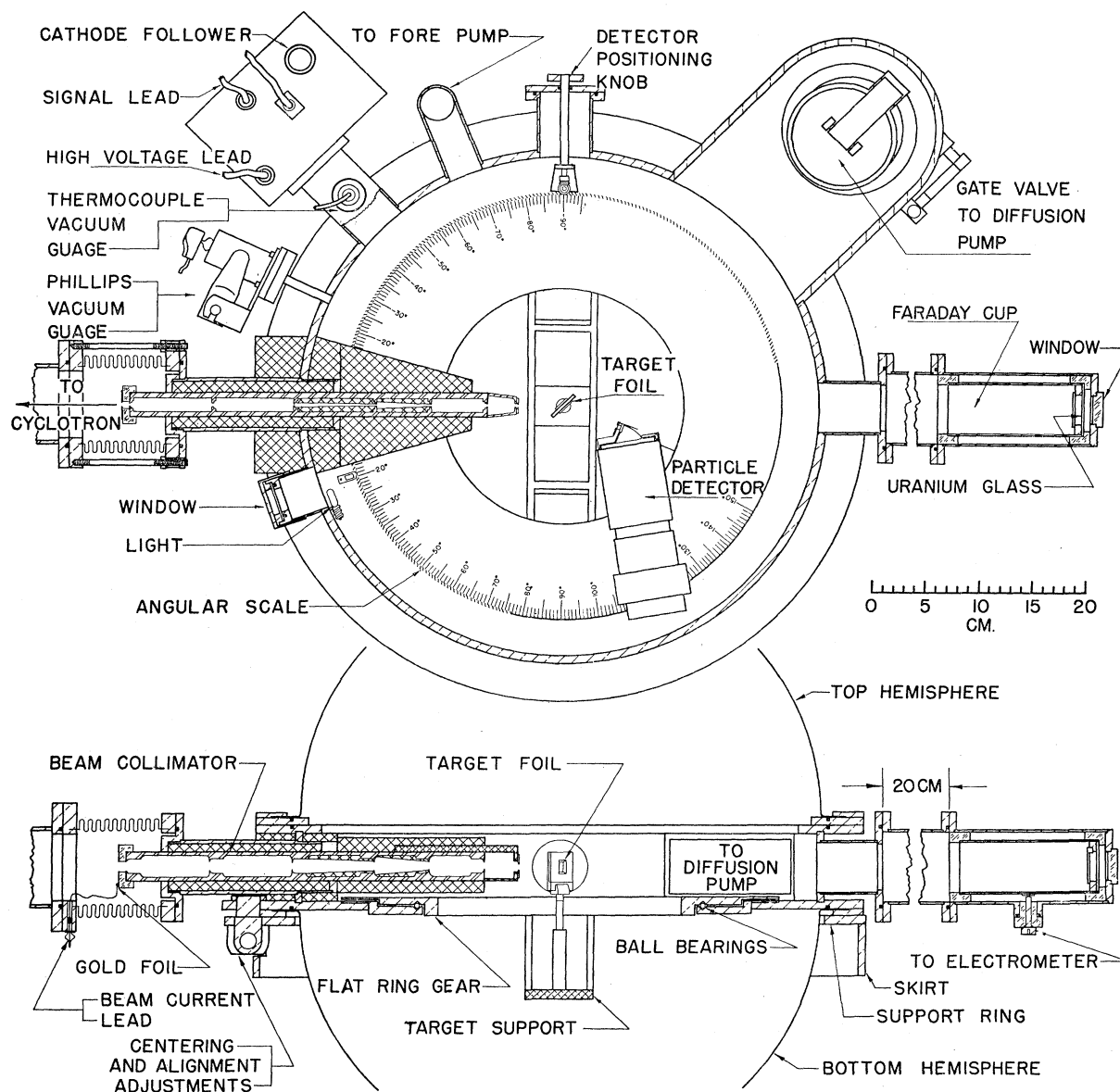


FIG. 1. Top and right-end cross-sectional views of the reaction chamber.

the nuclei involved in the reactions. On the basis of the assignment of zero spin to the ground state of  $\text{Zn}^{68}$  and the shell model assignments<sup>8</sup> of  $p_{1/2}$  for the ground state and  $g_{9/2}$  for the 436-kev isomeric level of  $\text{Zn}^{69}$ , it must be assumed that when  $\text{Zn}^{68}$  is bombarded by deuterons,  $p$ -wave neutrons are captured leading to the ground state of  $\text{Zn}^{69}$  and  $g$ -wave neutrons leading to the 436-kev level. The proton distributions are hence expected to be characterized by momentum transfers of  $l_n=1$  for the ground state group and  $l_n=4$  for the group leaving  $\text{Zn}^{69}$  in its first excited state. Direct comparison can be made with the results of stripping theory

<sup>8</sup> M. Goldhaber and R. D. Hill, *Revs. Modern Phys.* **24**, 179 (1952).

by fitting to the experimental angular distributions Butler's theoretical expression using these values for the parameter  $l_n$ .

## II. EXPERIMENTAL APPARATUS AND PROCEDURE

### Deuteron Beam

A reasonably monoenergetic beam of 11.9-Mev deuterons was obtained by selecting a narrow swath of the main beam at the end of the  $180^\circ$  deflection channel of the University of Illinois cyclotron. The beam emerged from the cyclotron through a tube containing a remotely operated shutter and entered a deflecting magnet where it was bent through an angle of about  $37^\circ$ . By means of

a proton spin resonance device the magnetic field in the deflecting magnet was held constant to within 0.1 percent and provided additional energy selection as well as deflection. The deuteron beam which reached the reaction chamber, about  $4\frac{1}{2}$  meters from the cyclotron exit port, had a mean energy of 11.9 Mev and an energy spread of approximately  $\pm 50$  kev. The cyclotron was run continuously during data taking periods, and the beam was interrupted whenever necessary by operating the shutter in front of the deflecting magnet.

### Reaction Chamber

Top and right-end cross-sectional views of the reaction chamber are shown in Fig. 1. The center section of the chamber is a cylindrical shell of  $\frac{1}{4}$ -inch thick brass,  $19\frac{1}{2}$  inches in diameter and  $2\frac{1}{2}$  inches high. Spun aluminum hemispheres (about  $\frac{1}{32}$  inch thick) are used for the top and bottom. The top hemisphere is simply set in place on a rubber gasket in the upper flange of the cylindrical section and is easily lifted off to gain access to the inside. The chamber is supported by a tripod ring-stand which fits under the lower flange of the cylindrical section. Screw adjustments and a vertical shaft at the front of the ring permit translation of the front of the chamber in a direction perpendicular to the beam and rotation of the entire chamber about a vertical axis. Adjusting screws on the legs of the tripod provide for vertical positioning. The chamber is evacuated by a 100-liter/sec oil-diffusion pump backed up by a mechanical fore-pump.

### Collimation of the Beam

The part of the collimating system which is located at the front of the chamber consists of seven rectangular apertures. The first six of these were milled in two pieces of stainless steel which are fastened together to form a bar of one-inch-square cross section. Two machined channels, centered on the beam axis of the chamber about eight inches apart, position the bar along a diameter to within 0.5 minute of arc. The first aperture, which was milled out of gold sheet inlaid in the steel, serves to minimize the gamma ray background by excluding divergent beam as far in front of the chamber as possible. The third (also of gold), together with the aperture at the exit of the deflecting magnet, defines the cross section and divergence of the primary beam which passes through the chamber. The other five apertures serve to limit the spray of particles scattered from the defining slit and the inside of the collimator. The final aperture, located about 4 cm from the target foil, is adjustable and mounts in a Dural frame which is fastened to the end of the steel bar.

The primary beam has a maximum divergence (half-angle) within the chamber of 13.5 minutes and a measured cross-sectional area at the target position of  $1.6\text{ mm} \times 6.8\text{ mm}$ . In the plane of the particle detector the maximum half-angle of spray is 21 minutes for

particles which have scattered once within the collimation system and  $3^\circ$ –20 minutes for particles which have scattered twice. A considerable decrease in the background gamma radiation at low angles was achieved by filling the spaces between slits with lead wherever possible.

### The Target Holder

The target foil is mounted in a frame at the center of the chamber, the intersection of the beam with the foil defining the target volume. The frame, which slips into a groove accurately milled in position along a diameter of the chamber, may be removed from the chamber for convenience in loading target foils. For detector angles in the range from  $0^\circ$  to  $90^\circ$  the plane of the target is set at  $45^\circ$  to the beam direction (as shown in Fig. 1). For detector angles greater than this the foil holder is rotated  $90^\circ$ .

### The Particle Detector

A scintillation crystal and a selected RCA 5819 photomultiplier tube are used to detect particles emitted by the target. A NaI(Tl) crystal of approximate dimensions  $6\text{ mm} \times 9\text{ mm} \times 0.8\text{ mm}$  is mounted in a channel near the end of a Lucite light pipe (Fig. 2). The Lucite is curved in such a way that the light from the crystal which strikes its inside surface is totally reflected toward the photocathode of the tube. The light pipe is joined to the multiplier tube by a strip of aluminum foil cemented to both members with Duco cement. The intervening space is filled with Dow Corning 703 fluid, a clear, thin, low vapor pressure oil, which optically couples the Lucite to the glass photomultiplier tube and minimizes light losses due to internal reflections. Crystals were freshly cleaved in a jet of dry helium immediately before mounting and were covered by  $0.16\text{ mg/cm}^2$  aluminum foil as soon as they were in place on the light pipe.

A rectangular slit defines the solid angle, and a Lucite absorber immediately in front of the crystal attenuates the energy of the incident particles. The slit has the dimensions  $1.60\text{ mm} \times 6.35\text{ mm}$  and is situated 5.4 cm from the center of the target. Absorbers used in the

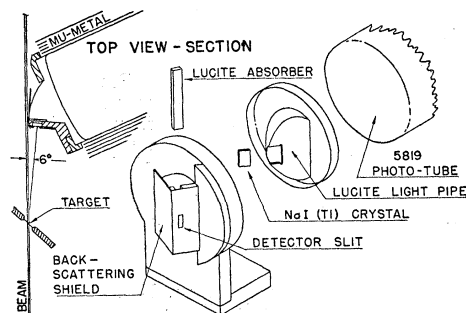


FIG. 2. Top cross-sectional and exploded isometric views of the particle detector.

present work were sufficiently thick to completely stop elastically scattered deuterons and low energy protons.

The detector is fastened to a ring-gear which is supported by ball bearings and can be rotated about a vertical axis through the center of the target by means of a shaft which passes through an O ring seal in the side of the chamber. The angular position of the detector slit can be read from a scale which is scribed on the ring-gear and is visible through a window near the front of the chamber. At angles lower than about  $6^\circ$  the side of the detector intercepts the main beam. At high angles the collimating system acts as a stop and limits the maximum detector angle to about  $120^\circ$ .

A cylindrical shell of several thicknesses of annealed mu-metal shields the photomultiplier tube from external magnetic fields. Electrical connections to the tube consist of a high voltage lead, a ground wire, and a signal lead, all of which pass through Stupakoff seals and terminate in a shielded box on the side of the chamber. A Higinbotham +500–1500-volt supply<sup>9</sup> is used for the high voltage, and positive signals from the last dynode of the photomultiplier tube are amplified by a Los Alamos model 100 pulse amplifier.<sup>10</sup>

### Charge Collection and Measurement

A Faraday cup is supported by Lucite rings in a tube connected to the rear of the chamber along the beam axis. The rear of the cup is made of uranium glass and is shielded from the direct beam by a hinged sheet of mu-metal which can be raised by means of an external magnet. This construction provides a convenient means for checking the alignment of the chamber or estimating the thickness of target foils by noting the size of the beam spot on the uranium glass. The cup was electrically connected to two precision one-microfarad polystyrene condensers which were connected in parallel. The voltage across the condensers, as measured by a vibrating reed electrometer,<sup>11</sup> provided a measure of the integrated beam through the chamber during the 3 to 10 minute runs taken at each angle.

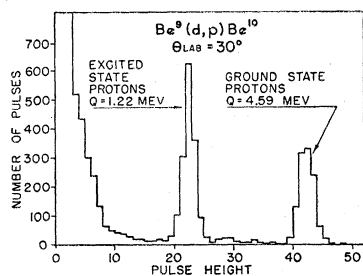


FIG. 3. Pulse height spectrum of protons from  $(d,p)$  reactions on  $\text{Be}^9$  at a laboratory angle of  $30^\circ$ .

<sup>9</sup> W. A. Higinbotham, Rev. Sci. Instr. **22**, 429 (1952).

<sup>10</sup> W. C. Elmore and M. Sands, *Electronics* (McGraw-Hill Book Company, Inc., New York, 1949).

<sup>11</sup> Palevsky, Swank, and Grenchik, Rev. Sci. Instr. **18**, 298 (1947).

### Pulse Recording and Discrimination

Since protons belonging to several different energy groups were simultaneously incident on the detector, it was necessary to perform a pulse height analysis in order to decompose the spectrum and obtain information on particles of a single energy group. This was done photographically. An oscillograph record camera (Du Mont type 314) employing 100-ft lengths of 35-mm film was used to record the signals on the cathode ray tube of a triggered sweep oscilloscope (Tektronix 511A). The signals were traced on the face of the tube parallel to an illuminated Lucite scale containing 100 equally spaced pulse-height divisions. Since the film ran continuously, the image of the scale on the film consisted of 100 equally spaced lines running the length of the film superimposed on the images of the pulses. For analysis, the films were projected on the screen of a micro-film reader (Diebold "Flowfilm") and magnified by a factor of about 18. When the particle groups were cleanly resolved, it was necessary only to count the pulses within the separated groups. For groups which were not resolved, the number of pulses whose peaks lay in each of the separate channels, was determined by counting the 10 channel swaths across the film. The use of a keyboard with 10 keys, each connected to a mechanical register, made it possible to read the films and sort the pulses at an average rate of about 2000 pulses an hour.

### Determination of Foil Thickness

A thin-window, argon-filled ionization chamber and a Po alpha source were used to determine the air equivalent thickness of each target foil. The foil to be measured was interposed between the alpha source and the window of the ionization chamber and the pulse heights from the chamber noted. Upon withdrawal of the foil the alpha source was removed a distance equal to the air equivalent thickness of the foil in order to restore the pulse heights to their former level. In terms of the energy equivalent for 11.9-Mev deuterons the foils used in the present work had thicknesses of less than 50 kev.

### III. $(d,p)$ REACTIONS ON $\text{Be}^9$

Deuterons of 11.9 Mev were directed at a  $0.43 \text{ mg/cm}^2$  free foil of beryllium metal,<sup>12</sup> and the reaction protons associated with the ground state and first excited state of  $\text{Be}^{10}$  were detected at 22 angles between  $5^\circ$  and  $85^\circ$ . Different absorber thicknesses were used in front of the crystal in each of three overlapping angular intervals. Absorbers were chosen of sufficient thickness to absorb completely the elastically scattered deuterons and to reduce the energy of the protons from the excited state group to about 5 or 6 Mev.

<sup>12</sup> The Be foil was generously sent to us several years ago by Dr. Hugh Bradner of the University of California. See H. Bradner, Rev. Sci. Instr. **19**, 662 (1948).

Figure 3 shows a number *versus* pulse height plot for a laboratory angle of  $30^\circ$ . After the absorber, the energies of the protons in the two groups shown are 11.7 and 6.3 Mev. The small pulse heights are due to gamma rays and are present to about the same extent with or without a target foil. More than half of the gamma-ray counts result from the high background in the experimental area when the cyclotron is accelerating deuterons. The rest originate in the collimator or the Faraday cup when the beam passes through the chamber. The large pulse heights not included in the peaks are due mostly to protons from the Lucite absorber, which are knocked into the crystal by neutrons from the competing  $\text{Be}^9(d,n)\text{B}^{10}$  reaction.

Figure 4 shows the angular distributions in center-of-mass coordinates for the proton groups associated with the ground state and the 3.37-Mev excited state of  $\text{Be}^{10}$  along with theoretical curves calculated from Butler's expression with  $l_n=1$  and  $r_0=5.1 \times 10^{-13}$  cm. The vertical lines through the experimental points are standard deviations based on the number of counts at each angle. The discrepancies shown in Fig. 4 between the theoretical curves and the experimental points are typical of distributions characterized by  $l_n=1$ . It is frequently the case, as has been noted by other workers,<sup>13</sup> that the agreement between theory and experiment is rather poor for  $l_n=1$  distributions. Previously reported results have indicated that when the principal maximum occurs at angles lower than about  $15^\circ$  and the theoretical curve is constructed to have the same maximum value as the experimental peak, the best possible fit to the data becomes progressively poorer the lower the angle of the peak. The theoretical curves appear to be somewhat broader than the experimental distributions and are displaced toward smaller angles. The discrepancies between the experimental points and the theoretical curves in Fig. 4 are consistent with this trend.

A comparison of the distributions obtained from the  $\text{Be}^9(d,p)\text{Be}^{10}$  reactions for different incident deuteron energies indicates that as the energy is increased the secondary maximum decreases in size relative to the primary and shifts toward smaller angles, eventually merging with the primary maximum. The work of El-Bedewi<sup>2</sup> at 7.7 Mev shows a well defined secondary maximum in the ground state distribution at about  $75^\circ$  to  $80^\circ$ . This peak is much less prominent in the present work, and in the distribution reported by Black<sup>4</sup> at 14.5 Mev it appears to have coalesced with the primary peak. Only a small secondary maximum seems to be present in the excited state distribution at 7.7 Mev, and it is not apparent at all in the present work or at 14.5 Mev. As the deuteron energy is increased the shape of the proton distribution becomes similar to that sug-

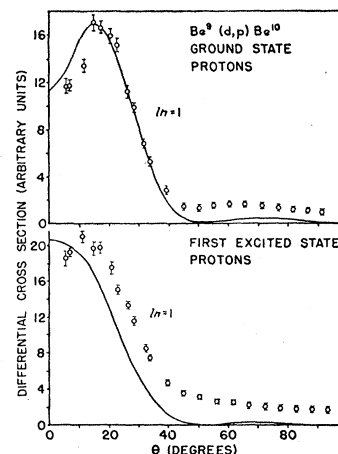


FIG. 4. The angular distributions of protons associated with the ground state and the first excited state of  $\text{Be}^{10}$  in the reaction  $\text{Be}^9(d,p)\text{Be}^{10}$  for a deuteron energy of 11.9 Mev. Solid curves were calculated from Butler's theory with  $r_0=5.1 \times 10^{-13}$  cm.

gested by Daitch and French,<sup>14</sup> in which the zero in Butler's curve is not present and the distribution decreases monotonically with angle, at least up to  $90^\circ$ .

#### IV. $(d,p)$ REACTIONS ON $\text{N}^{14}$

A foil target containing nitrogen (99.6 percent  $\text{N}^{14}$ ) was produced by vacuum evaporating a small quantity of a nitrogen-rich compound, and collecting the vapor on a thin, freshly prepared zapon film. The compound 1-cyano-guanidine ( $\text{C}_2\text{H}_4\text{N}_4$ ), in the form of small white flakes was sublimed from a wolfram boat electrically heated to dull red in a vacuum of  $10^{-5}$  mm Hg. The resulting target consisted of a  $0.5 \text{ mg/cm}^2$  thickness of guanidine deposited on the zapon film backing (estimated thickness,  $0.02 \text{ mg/cm}^2$ ). Protons associated with the ground state and doublet first excited state (doublet separation about 30 kev) were counted at angles between  $6^\circ$  and  $90^\circ$  using absorbers sufficiently thick to completely stop elastically scattered deuterons and hydrogen nuclei from the target foil. Protons from the ground state carbon reaction  $\text{C}^{12}(d,p)\text{C}^{13}$  are less energetic than protons associated with the  $\text{N}^{15}$  doublet level by about 600 kev. The carbon component of the target caused no difficulty except at low angles where, due to their great preponderance and the limited resolution of the detector, the pulses in the carbon group tended to spill over into the nitrogen peak and cause considerable uncertainty in the determination of the number of nitrogen pulses. Figure 5 shows pulse height spectra observed at laboratory angles of  $6^\circ$  and  $45^\circ$ .

The angular distributions of protons leading to the ground state and the first excited state of  $\text{N}^{15}$  are shown in Fig. 6. The vertical lines represent standard deviations based on the number of counts at each angle except for low angle points in the excited state distribution for which the uncertainties arising from the possible confusion with pulses from the carbon reaction are also included. The ground state proton group has a distri-

<sup>13</sup> See reference 3. See also the review article by R. Huby in the book edited by O. R. Frisch, *Progress in Nuclear Physics* (Pergamon Press Ltd., London, 1953), Vol. 3, Sec. 7.

<sup>14</sup> P. B. Daitch and J. B. French, *Phys. Rev.* **87**, 900 (1952).

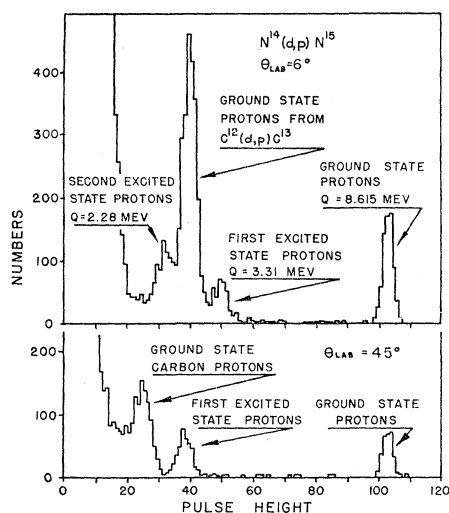


FIG. 5. Pulse height spectrum of protons from  $(d,p)$  reactions on  $N^{14}$  at laboratory angles of  $6^\circ$  and  $45^\circ$ .

bution characteristic of a momentum transfer  $l_n=1$  in agreement with the work of Gibson and Thomas<sup>5</sup> at a deuteron energy of 8 Mev, and a reasonably good fit to the data is achieved using Butler's expression with  $r_0=5.8 \times 10^{-13}$  cm. In the work at 8 Mev the distribution of the protons leaving  $N^{15}$  in its doublet first excited state showed no forward maximum. Hence, it has been inferred that the reaction takes place predominately by compound nucleus formation and that the levels have large spins. Since the present work shows a distinct maximum at low angles, it appears that the conclusion that the levels have large spins is probably not correct. In view of the large uncertainties in the low angle data, no definite statement can be made as to the spins of the levels or the momentum transfers involved. It seems possible, however, that bombarding with deuterons of higher energy might give rise to a distribution that is more typical of those from reactions which take place primarily by the stripping process.

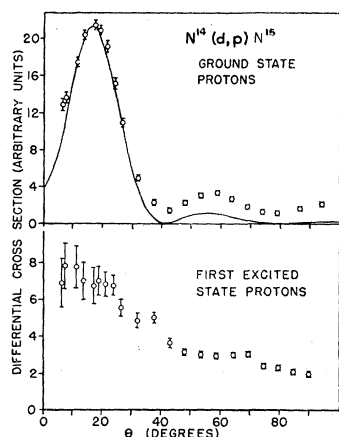


FIG. 6. The angular distribution of protons associated with the ground state and the first excited state of  $N^{15}$  in the reaction  $N^{14}(d,p)N^{15}$  for a deuteron energy of 11.9 Mev. Solid curve was calculated from Butler's theory with  $r_0=5.8 \times 10^{-13}$  cm.

## V. $(d,p)$ REACTIONS ON $Zn^{68}$

Targets were prepared by electrodepositing zinc metal, highly enriched in  $Zn^{68,15}$  on thin metallic backings. Gold leaf and evaporated foils of copper were used as backing materials and both  $Zn(CN)_2$  and  $ZnSO_4$  were used as plating solutions. The proton spectrum was found to be the same for all of the targets, except that the copper backing gave a background approximately 20 times higher than the gold backing and a large contribution from carbon and nitrogen reactions occurred when the cyanide solution was used in plating, probably due to the presence of the AuCN which was formed.

The energies of the protons associated with the ground state and the second excited state of  $Zn^{69}$  were obtained by comparing their pulse heights with pulse heights due to protons of known energies from other reactions. Several different target materials were mounted in a foil holder whose position could be adjusted from outside the chamber. Pulse heights due to protons from reactions on  $Be^9$ ,  $C^{12}$ ,  $O^{16}$ ,  $Al^{27}$ , and  $Zn^{68}$  were observed in succession and time exposures taken of the oscilloscope traces. Three sets of measurements were made at different detector angles and on different days. In each case photographs were taken of pulse heights due to protons from zinc targets and three or four other target materials. The unknown proton energies were obtained from curves of pulse height *versus* energy which were constructed using the pulses from protons of known energy.  $Q$  values for the reactions were calculated for each of the three energy determinations, and the resulting values averaged to give  $Q=4.16 \pm 0.15$  Mev for the reaction leading to the ground state of  $Zn^{69}$  and  $Q=3.39 \pm 0.15$  Mev for the second excited state. The  $Q$  value for the ground state reaction agrees within experimental accuracy with the value  $4.39 \pm 0.25$  Mev which can be calculated from the measured masses<sup>16,17</sup> of  $Zn^{68}$  and  $Ga^{69}$  and Duffield and Langer's<sup>18</sup> values for the beta spectrum end point.

The spectrum of protons emitted by the target was observed at 23 angles between  $7\frac{1}{2}^\circ$  and  $90^\circ$ . Two different targets were used in the distribution measurements: a thin target ( $0.64$  mg/cm<sup>2</sup> of Zn) for angles up to  $60^\circ$ , and a thick target (about  $5$  mg/cm<sup>2</sup> of Zn) for higher angles. Both targets were plated on  $0.2$  mg/cm<sup>2</sup> gold leaf from solutions of  $ZnSO_4$ . A Lucite absorber  $1.7$  mm thick was used in front of the detector at all angles.

Figure 7 shows, for 4 different angles, the pulse

<sup>15</sup>  $ZnO$  containing an isotopic abundance of 95.5 percent  $Zn^{68}$  was obtained on a loan basis from the Electromagnetically Enriched Isotopes Inventory of the Oak Ridge Laboratory of the Atomic Energy Commission by Professor R. D. Hill, to whom the author is indebted for making a quantity available for the present work.

<sup>16</sup> Collins, Nier, and Johnson, Phys. Rev. **86**, 408 (1952).

<sup>17</sup> B. G. Hogg and H. E. Duckworth, Phys. Rev. **92**, 848(A) (1953).

<sup>18</sup> R. B. Duffield and L. M. Langer, Phys. Rev. **89**, 854 (1953).

height distribution arising from protons which leave  $\text{Zn}^{69}$  in its ground state and excited states at 436 kev, 770 kev, and 1.6 Mev (denoted in the figure as Zn I, II, III, and IV, respectively). Protons in the peak Zn I have a laboratory energy of about 16 Mev at  $7^\circ$ . The low-angle spectrum illustrates the strong  $Z$  dependence of  $(d,p)$  reaction cross sections. The  $0.2 \text{ mg/cm}^2$  of gold contributed only a few counts, while the  $0.64 \text{ mg/cm}^2$  of Zn accounted for two large peaks. The highest peak, two and one-half times as high as the peaks from the Zn reactions, was caused mostly by a small carbon contaminant. The main source of the carbon was probably vacuum pump oil, and the contamination increased steadily while the beam was on. This possibly could have been avoided by more effectively baffling the pump or by using a liquid air trap in the pumping system. The pulse height distributions were corrected for the background due to the gold backing material which was found in an independent

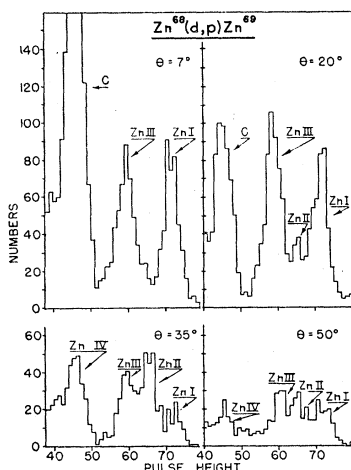


FIG. 7. Pulse height spectrum of protons from  $(d,p)$  reactions on  $\text{Zn}^{68}$  at laboratory angles of  $7^\circ$ ,  $20^\circ$ ,  $35^\circ$ , and  $50^\circ$ .

measurement. Protons from the gold accounted for less than 4 percent of the counts observed in the region of interest at any angle.

For the purpose of decomposing the number *versus* pulse height histograms into contributions from the individual groups (Zn I, II, and III), it was assumed that each of the groups gives rise to a normal "Gaussian" distribution of pulse heights whose root-mean-square width (standard deviation) is the same for each of the groups and is independent of angle. The value of the root-mean-square width was found from the reasonably well resolved individual peaks which are present in the low angle data by taking the second moments of the distributions and applying the parallel axis theorem. The separations of the centers of the assumed normal curves were taken as the weighted average values of the separations of the peaks in the histograms which were estimated at each angle. Using these values for the root-mean-square width and the separations of the centers, the amplitudes of the three assumed normal

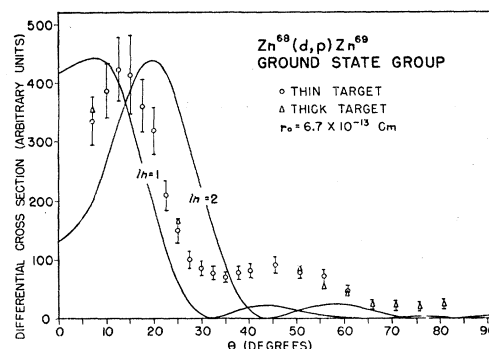


FIG. 8. The angular distribution of protons associated with the ground state of  $\text{Zn}^{69}$ . Solid curve was calculated from Butler's theory.

curves were calculated by fitting smooth curves to the number *versus* pulse height histograms by the method of averages.<sup>19</sup> A 24-channel range in pulse heights was used, and, in essence, the number of counts in each channel was equated to the sum of contributions from three normal distributions with unknown coefficients. At each angle the 24 linear algebraic equations so obtained were grouped into three sets and the equations in each set added to give three equations which were solved for the unknown coefficients (amplitudes of the component normal distributions).

Plots of the angular distributions of the proton groups leading to the ground state and to the 436-kev excited level of  $\text{Zn}^{69}$  are shown in Fig. 8 and Fig. 9, respectively. Figure 10 shows the distribution of the protons which leave the final nucleus with an excitation of 770 kev. The uncertainties drawn through the experimental points indicate the combined root-mean-square errors associated with the counting statistics and the calculation of the amplitudes of the assumed normal distributions from the pulse height histograms as determined by a detailed error analysis of the calculation. At least two runs were made at each angle below  $60^\circ$ , and the

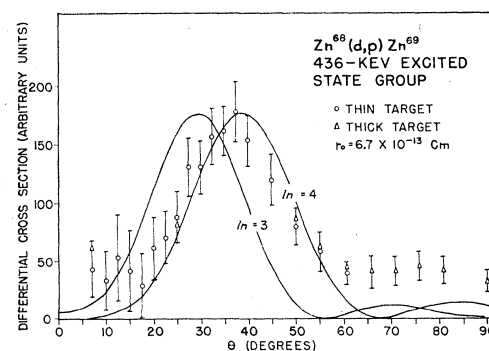


FIG. 9. The angular distribution of protons associated with the 436-kev excited level of  $\text{Zn}^{69}$ . Solid curve was calculated from Butler's theory.

<sup>19</sup> See, for example, J. B. Scarborough, *Numerical Mathematical Analysis* (The Johns Hopkins Press, Baltimore, 1950).

data were analyzed separately. The experimental points shown in the figures are weighted average values obtained from all of the data at each angle. The data obtained using a thick target, were normalized to the thin-target data, as indicated in the figures, at five points below  $65^\circ$ . No determination of the angular distribution was attempted for the group Zn IV since it was largely obscured by the ground state group from the carbon contaminant.

The value of  $r_0$  used in the calculation of the Butler curves in Figs. 8, 9, and 10 corresponds to the nuclear radius plus the range of nuclear forces as obtained from fast neutron scattering experiments and was calculated from the general expression given by Gamow and Critchfield,<sup>20</sup>  $r_0 = (1.22A^{1/3} + 1.7) \times 10^{-13}$  cm. In agreement with the predictions mentioned earlier, the data shown in Figs. 8 and 9 are best fitted by theoretical curves with  $l_n = 1$  for the ground state group and  $l_n = 4$  for the 436-keV isomeric level. The momentum transfers obtained from an analysis of the proton distributions in terms of Butler's stripping theory are hence consistent with the level assignments inferred from shell theory and supported by the  $M4$  character of the radiation from the 436-keV level, the allowed beta-decay of the ground state of  $\text{Zn}^{69}$ , and the measured spin of the

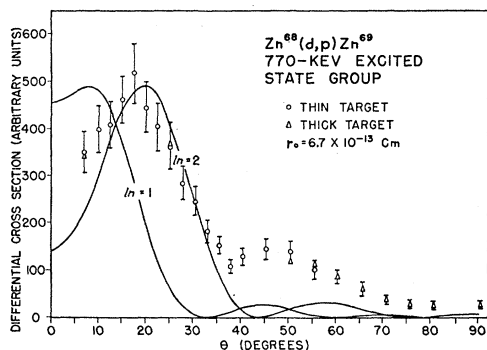


FIG. 10. The angular distribution of protons associated with the 770-keV excited level of  $\text{Zn}^{69}$ . Solid curve was calculated from Butler's theory.

<sup>20</sup> G. Gamow and C. L. Critchfield, *Theory of Atomic Nucleus and Nuclear Energy-Sources* (Clarendon Press, Oxford, 1950).

ground state of  $\text{Ga}^{69}$ . The data shown in Fig. 10 are in reasonable agreement with a theoretical curve using  $l_n = 2$ . The relatively large intensity of this group suggests that it is associated with a single particle level. A level assignment consistent with the shell model would require that the captured neutron go into the  $d_{5/2}$  orbit in the next higher shell. Somewhat better fits to the experimental data for the excited state groups can be obtained by taking  $r_0 = 7.1 \times 10^{-13}$  cm.

A rather unexpected feature of these distributions is the relatively large intensities of the groups associated with high momentum transfers. The calculations of Butler have indicated that, other factors being equal, the magnitude of the peak in the angular distribution should decrease with increasing values of  $l_n$  by about an order of magnitude as  $l_n$  is increased by 2. Previously reported experimental results for a number of reactions involving target nuclei having mass numbers of 40 and lower<sup>3</sup> have, in general, shown this behavior. In the case of reactions on  $\text{Zn}^{68}$ , however, the observed ratio of the heights of the peaks for distributions having  $l_n = 4$  and  $l_n = 1$  is about 40 percent, and the peak in the  $l_n = 2$  distribution is about 25 percent higher than the peak in the  $l_n = 1$  distribution. Angular distributions obtained by Holt and Marsham<sup>7</sup> from the reaction  $\text{Sr}^{88}(d,p)\text{Sr}^{89}$  also show peaks associated with high  $l_n$  values which have much larger relative intensities than would be expected from the theoretical calculations. It appears that the predicted dependence of the magnitude of the peaks on  $l_n$  is unreliable for reactions involving heavy nuclei, and that stripping theory can in some cases be used in the interpretation of the angular distributions from reactions on heavy nuclei in which relatively high momentum transfers are involved.

The author wishes to acknowledge his indebtedness to the members of the cyclotron group and the cyclotron shop for their cheerful cooperation and assistance. A debt of gratitude is due Professor W. K. Jentschke, who supervised this work, for his valuable advice and constant encouragement. The author is particularly grateful to Professor R. D. Hill for suggesting  $\text{Zn}^{68}$  as a suitable target nucleus and for his generous assistance and encouragement and to Professor G. F. Chew for helpful discussions of the theoretical aspects of the work.